Optimal Resolution of State Space in Chaotic Hyperbolic 2-dimensional Maps

Gable M. Wadsworth and Daniel T. Kovari
(Dated: May 1, 2012)

Noise is a factor in every physical system. To deal with this physical constraint and better understand it, we seek to partition the state space of the system at some optimal resolution. The distribution we examine is stretched and contracted as the chaotic dynamics evolve and the noise results in a smearing of the distribution. We begin by examining weak noise as applied to a one dimensional quadratic map. Methods for partitioning two dimensional state spaces are outlined using "Knead and Fold" type maps. Periodic orbits are found for these maps and the evolution of noise along these cycles is examined using the Fokker-Planck operator. More interesting dynamics are explored in a 2-dimensional quadratic map which approximates the Hénon map. This map is chaotic and hyperbolic.

INTRODUCTION

Noisy systems are encountered everywhere. Physically, noise manifests itself throughout nature, often in the form of Brownian motion. Although deterministic systems are by definition free from stochastic noise, numerical approximations like rounding and truncation can also result in behaviors that are analogous to noise. The work presented in this paper is an exploration of the *optimal partition hypothesis* by Lippolis and Cvitanović[1, 2]. The hypothesis is briefly stated as follows.

For many deterministic systems, the state space over which they act can be partitioned into arbitrarily small regions which define a set of points that are all characterized by some recognizable behavior. The presence of noise in such systems tends to randomly kicks points in state space as they are propagated forward in time. As a result, at some level of revision, a partition will shrink beyond the point at which it is distinguishable from some neighboring partition. The *optimal partition hypothesis* can be stated as follows. If we consider a periodic orbit point to be representative of a partition and its measure (zeroth-order eigenvalue) to be characteristic of its "resolution", we can setup a *Rayleigh*-like criterion which determines if two periodic orbits are distinguishable and consequently whether their respective partitions are distinguishable.

NOISE

The interplay between deterministic dynamics and weak noise is quite interesting. While deterministic maps and equations of motion dictate the behavior of individual state space trajectories, the Perron-Frobenius operator can be used to describe the behavior of distributions of trajectories[3]. Imagine a gaussian state space probability distribution. Noise acts on the gaussian distribution by smearing the distribution as the system evolves. Conveniently, the Fokker-Plank equation can be used to determine how probability distributions evolve[4].

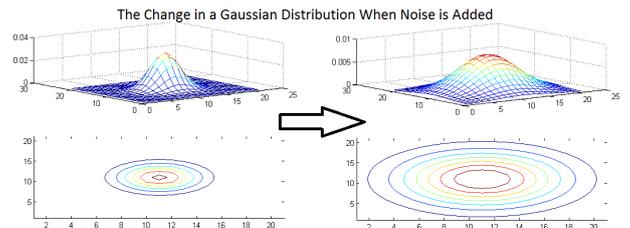The noise acts at each iteration of a map, $f(x) : x_n \to$

FIG. 1: Evolution of a gaussian distribution, starting with a $\sigma^2 = 10$ and then adding a diffusion tensor $D = 10$ so that $\sigma^2 + D = 20\hat{I}$. The gaussian undergoes stretching and the information in the distribution is thereby smeared.

x_{n+1}. For weak noise there is a Fick's current law,

$$j_i = \rho v_i - D \frac{\partial \rho}{\partial x_i} \tag{1}$$

To derive the Fokker-Planck equation we look at the result for the divergence theorem and insert it in the equation,

$$\partial_t \rho = -\partial_i j_i. \tag{2}$$

To evolve the system forward in time we look at the Fokker-Planck equation,

$$\partial_t \rho(x,t) + \nabla \cdot (v(x)\rho(x,t)) = D\nabla^2 \rho(x,t) \tag{3}$$

Analogous to the Perron-Frobenius operator (P-F), the Fokker-Planck operator (F-P) evolves a system forward.

$$\mathcal{L} \circ \rho(x) = \int [dy] e^{-\frac{(x - \Lambda y)^2}{4D}} \rho(y) \tag{4}$$

The critical difference between the two operators it that the delta-function in the P-F has been replaced by a gaussian, whose width corresponds to the amount of noise in the system.

Consistent with the P-F there is an adjoint (P-F),

$$\mathcal{L}^\dagger \circ \tilde{\rho}(x) = \int [dy] e^{-\frac{(\Lambda x - y)^2}{4D}} \tilde{\rho}(y) \tag{5}$$

The adjoint operator looks at the behavior of a distribution under reversed flow. Notice that the noise will continue to expand the distribution. The resolution with which we can look back to previous states will be limited by the amount of noise present[2].

MAPS

Periodic orbit theory provides a set of powerful computational tools for looking at chaotic flows. One way to approach the partitioning of state space is to use periodic orbits as representative templates for the behavior of the partition in which they are members[3]. Consider a 1-dimensional return map:

$$x_{n+1} = f(x_n). \tag{6}$$

In the case of a unimodal map, the state space lends itself to being partitioned into two regions: values left of the extrema and those to the right (0,1 respectively). These partitions can be further refined by sub-dividing them into regions that describe their future behavior under iterations of the map. Symbolically, we can use binary sequences to represent the history/destiny of a cycle. Further revisions result in labels of increased length.

$$0 \rightarrow \begin{cases} 01 \\ 00 \end{cases} \rightarrow \begin{cases} 011 \\ 010 \\ 001 \\ 000 \end{cases} \rightarrow \cdots \tag{7}$$

Each partition contains a point on periodic orbit, whose behavior typifies the behavior of the entire partition. In other words, the behavior of all the points within a partition will approximate the behavior of the associated periodic orbit.

Fokker-Plank of Periodic Orbits

The representative nature of periodic orbits provides a convenient method of analyzing the behavior in the partitions under the action of Fokker-Plank operator. The following is discussed in detail in the referenced papers by Cvitanović and Lippolis [1, 2]. A noisy linear map has the form:

$$x_{n+1} = \Lambda x_n + \eta_n, \tag{8}$$

where η_n is the contribution of gaussian white noise with variance 2D. For such maps F-P becomes the equation, 4

For contracting maps (i.e. $|\Lambda| < 1$) the unit eigenfunction of the operator is

$$\begin{aligned} \rho_0(x) &= N^{-1}e^{-x^2/2\sigma_0^2}, \\ \sigma_0^2 &= 2D/(1 - \Lambda^2), \end{aligned}$$

$$N = (4\pi D)^{1/2} \tag{9}$$

Likewise, for expanding maps the adjoint F-P has the unit eigenfunction:

$$\rho_0(x) = N^{-1}e^{-x^2/2\sigma_0^2}, \quad \sigma_0^2 = 2D/(\Lambda^2 - 1) \tag{10}$$

Applying a WKB-like approximation to the operator, it can be shown that an initial gaussian density

$$\rho_0(x_a + z_a) = c_a e^{-z_a^2/2\sigma_a^2} \tag{11}$$

about some point x_a, is transformed to

$$c_{a+1}e^{\frac{-z_{a+1}^2}{4D+2(f'_a)^2\sigma_a^2}} \tag{12}$$

by the (forward) operator, and to

$$c_{a-1}e^{\frac{-(f'_{a-1})^2 z_{a+1}^2}{4D+2\sigma_a^2}} \tag{13}$$

by the adjoint operator.

When considering the shape of the resulting gaussian distribution, one can see that the variance is described by the recursion relationships:

$$\sigma_{a+1}^2 = 2D + (f'_a\sigma_a)^2, \quad forward\,op.$$

$$(f'_{a-1}\sigma_{a-1})^2 = \sigma_a^2 + 2D, \quad adjoint\,op. \tag{14}$$

For a n-length periodic orbit point $\sigma_a = \sigma_{a+n+1} = \sigma_{a-n-1}$ and is therefore given by the formulas

$$\sigma_a^2 = \frac{2D}{1 - (f_a^{n'})^2}(1 + \sum_{i=1}^{n-1}(f_{a+1}^{n-i'})^2), \quad forward$$

$$\sigma_a^2 = \frac{2D}{1 - 1/(f_a^{n'})^2}(\frac{1}{(f'_a)^2} + ... + \frac{1}{f_a^{n'}}), \quad adjoint$$

$$f_{a+j}^{n'} = \prod_{i=j}^{n\pm1} f'_{a\pm i} \tag{15}$$

OPTIMAL PARTITION HYPOTHESIS

Armed with the equations from the previous section[15], we have an integral-free way of finding the zeroth-order eigenfunction of the Fokker-Plank operators at any periodic point in a map. We can then use that function as a measure of the for the behavior of the map in the region near a periodic orbit.

FINDING OPTIMAL PARTITIONS

The root of the *optimal partition hypothesis* is that periodic orbits in noisy systems can be used to gauge the behavior of regions within a state space map. When trying to optimally partition a map, a natural place to begin is to find the periodic orbits.

Finding Periodic Orbits

One of our goals in this project was to provide a generalizable construct from which more complex (and hopefully useful) maps can be optimally partitioned. As discussed in Chaosbook Ch.13[3], there are a number of ways to find the periodic orbits of a return map. Perhaps the most naive method would be to simply solve the periodic recursion relations (e.g. $x = f(x)$, $x = f(f(x))$,...) using a standard Newton method. The problem, of course, is that such an algorithm would quickly be overwhelmed by the recursive (and therefore increasingly wiggly) nature of the equations defining long periodic solutions. An alternative method is to use a "multi-shooting" *Newton-Raphson* method, where an n-length periodic orbit is transformed into an n-dimensional relaxation problem.

$$ F(x) = F \begin{pmatrix} x_1 \\ x_2 \\ \vdots \\ x_n \end{pmatrix} = \begin{pmatrix} x_1 - f(x_n) \\ x_2 - f(x_1) \\ \vdots \\ x_n - f(x_{n-1}) \end{pmatrix} \rightarrow \begin{pmatrix} 0 \\ 0 \\ \vdots \\ 0 \end{pmatrix} \quad (16) $$

For this system each equation is of order $f(x)$ and therefore immune to the problems that a typical Newton search would face. The cost for choosing this method is that the algorithm requires n guesses, specifying locations close to each point along a periodic orbit.

Deterministic Partitions

This work was motivated by the idea that every partition contains a representative periodic orbit point. Therefore, some intuition regarding the boundaries of a map's partitions can be used to inform the initial guesses fed into the "multi-shooting" method.

Generally, determining partition boundaries may not always be tractable. However, the partitions of unimodal maps form a binary tree like structure which lends itself to "easy" computation. For these binary type maps, a partition will always be subdivided at the point that is projected to the boundary of its next partition. To understand this consider the a unimodal map with only the 2 core partitions $0, 1$. The 0 partition will be divided into the regions 00 & 01 at the position that maps to the boundary of the 1 partition. Similarly the 1 partition is divided at the location that maps to the boundary of the 0 partition. We can extend this algorithm to any sub-level by the recursion relationship

$$ x_w = f(x_{*w}), \quad (17) $$

solved near the boundary or the new partition's parent. Here, w is a label for a previously determined boundary and $*w$ is the label for the new partition. For example,
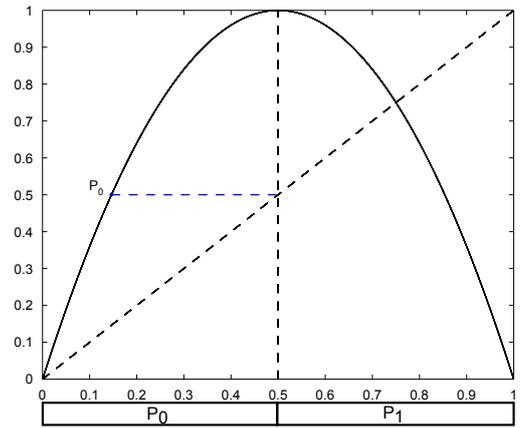

FIG. 2: Partitioned unimodal map. $x < 1/2 \rightarrow 0$; $x > 1/2 \rightarrow 1$
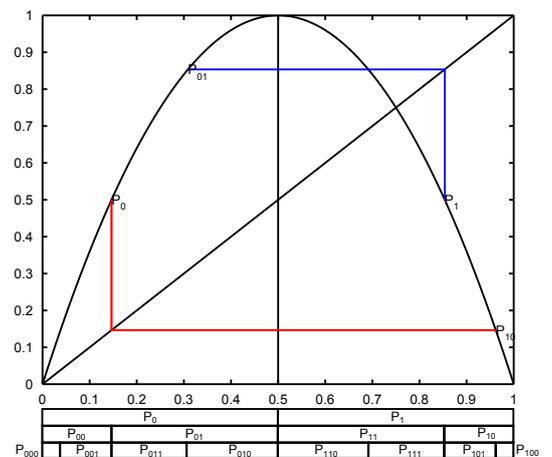

FIG. 3: Partitioned unimodal map. Partition boundaries found by looking for projection onto previous boundaries.

if $w = 01$ and $*w = 101$, the parent partition would be 10. In which case, the equation should be solved near x_{10}, which would have been generated by a previous iteration.

Fokker-Plank of n-Dimensional Orbits

Analogous to the above formulation, the n-dimensional Fokker-Plank operator can be linearly expanded around a point x_a as follows:

$$ \mathcal{L}_a(z_{a+1}, z_a) = \frac{1}{N} e^{-\frac{1}{2}(z_{a+1} - M_a z_a)^T \frac{1}{\Delta}(z_{a+1} - M_a z_a)} , $$

where Δ is the noise tensor, M_a is the Jacobian at point x_a with eigenvalues $\{\Lambda_0, \Lambda_1, ...\}$. Assuming the map is only contracting ($|\Lambda_i| < 1 \forall i$) or only expanding ($|\Lambda_i| > 1 \forall i$), the n-dimensional recursion relationship for the covariance matrix is:

$$ Q_{a+1} = M_a Q_a M_a^T + \Delta_a \quad |\Lambda| < 1 $$

$$Q_a = M_a Q_{a+1} M_a^T + \Delta_a \quad |\Lambda| > 1 \qquad (18)$$

For periodic orbits this results in the formula:

$$\begin{aligned} Q_a = \Delta_a &\ + \ M_{a-1}\Delta_{a-1}M_{a-1}^T + ... \\ &\ + \ M_{a-n}^n \Delta_{a-n}(M_{a-n}^n)^T \quad |\Lambda| < 1 \end{aligned}$$

$$Q_a = \Delta_{p,a} \ + \ M_{a-1}\Delta_{p,a}M_{a-1}^T + ... \quad |\Lambda| > 1 \quad (19)$$

$$where \ \Delta_{p,a} = \Delta_a + M_{a-n}^n \Delta_{a-n}(M_{a-n}^n)^T + ... \qquad (20)$$

These relationships do not hold up for points on a map that are hyperbolic (i.e. there are some expanding eigenvectors and some which are contracting). Typically, noise is not isotropic therefore the above equations cannot be easily diagonalized. However, in the case where the noise tensor Δ acts either uniformly or strictly along the eigenvector directions, the Fokker-Plank operator is separable and the above relationships are recoverable. These cases are discussed later in this paper.

OPTIMAL PARTITIONS

1-D Unimodal Maps

The quadratic unimodal map in one dimension can be written as,

$$x_{n+1} = 1 - 4(x_n - \frac{1}{2})^2 \qquad (21)$$

The map is run through several iterations of the outlined *optimal partition* algorithm. Periodic orbits are determined and their measures are checked for overlaps. Each figure[13, 14, 15, 4, 5] for the quadratic map only shows cycles of the length specified and no other cycles (the 0 cycle and 1 cycle consistently appear because they are fixed and the cycles are not checked to see if they are prime.) The first overlap is detected at cycle length 3 and the cycles 001 and 011[15] are subsequently pruned from the Markov chain. At cycles of length 5[5], all periodic orbits have overlapping gaussian distributions and the cycles with finest resolution are shown in the Markov chain diagram 6

2-D *Knead and Fold* Maps

As previously discussed, the general form of the linearized Fokker-Plank formulation fails for maps that are hyperbolic. However, in the case where noise is isotropic and acts only along the eigenvectors of the Jacobian of the map, there is a "work-around". For maps where there
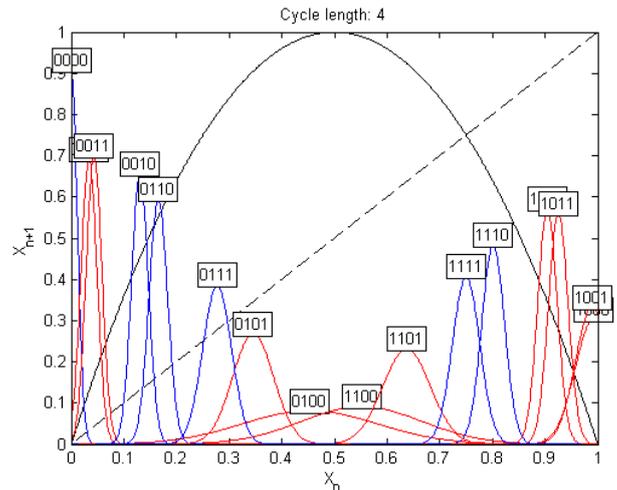

FIG. 4: For the fourth iteration of the code on the 1-dimensional quadratic map, the separation between cycles of length 4 begins to break down for cycles 001 and 011, which display some overlap.
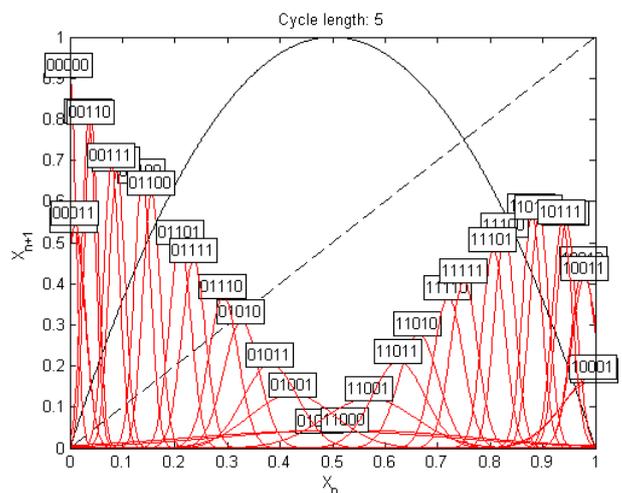

FIG. 5: For the fifth iteration of the code on the 1-dimensional quadratic map, the separation between cycles of length 5 breaks down completely and there is no further resolution possible.

are no off-diagonal terms in the Jacobian, isotropic noise results in a separable Fokker-Plank equation:

$$\begin{aligned} \mathcal{L}_a(z_{a+1}, z_a) = &\ \frac{1}{N} e^{-\frac{1}{4D}(z_{1,a+1} - M_{11}z_{1,a})^2} * \\ &\ e^{-\frac{1}{4D}(z_{2,a+1} - M_{22}z_{2,a})^2} * ... \end{aligned} \qquad (22)$$

Consequently, the recursion relationships characterizing the zeroth-order eigenvectors of the F-P [15] will still hold true, albeit only along the eigenvectors of the Jacobian.

To illustrate how this "diagonalization" type formulation could be applied we consider 2-D maps of the *knead-and-fold* variety. One of the simplest maps of this variety is the non-folded Baker's Map (a.k.a. Bernoulli shift),
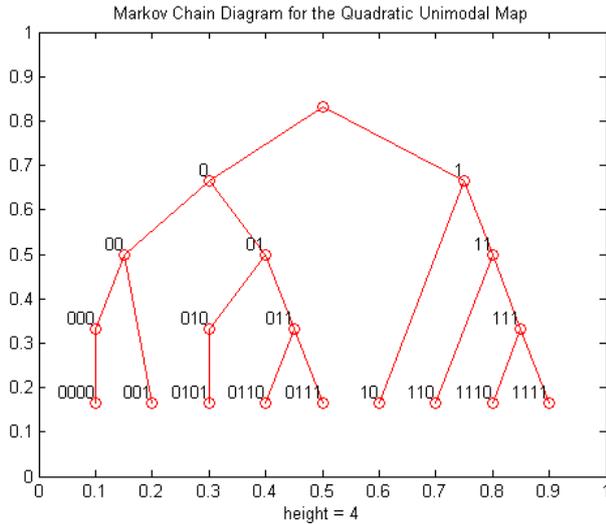
FIG. 6: Here it can be seen where the quadratic map is pruned based on the ability to resolve the state space in the presence of noise.
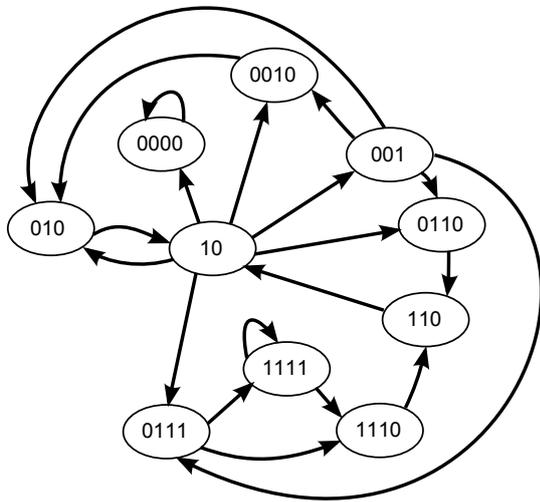

FIG. 7: Transition diagram for the 1-dimensional quadratic map with optimal partitions for noise $D = 0.001$.

pictured in figure 8.

The Baker's Map is represented by the set of equations,

$$x_{n+1}, y_{n+1} = \begin{cases} 2x_n, \frac{y}{2} & 0 \leq x \leq \frac{1}{2} \\ 2x_n - \frac{1}{2}, \frac{1}{2} + \frac{y_n}{2} & \frac{1}{2} < x \leq 1 \end{cases} \quad (23)$$

For maps of this type, the operation applied to the vertical coordinate (y) can be thought of as simply the inverse of the operation applied to the horizontal coordinate (x). As a result the vertical coordinate of a periodic point will simply be the horizontal coordinate of that point mirrored across the $y = x$ line (see figure 10).

Qualitatively, when noise is reasonably small, the map's partitions are very fine and very uniform. Imagine instead of labeling the sections with binary numbers,
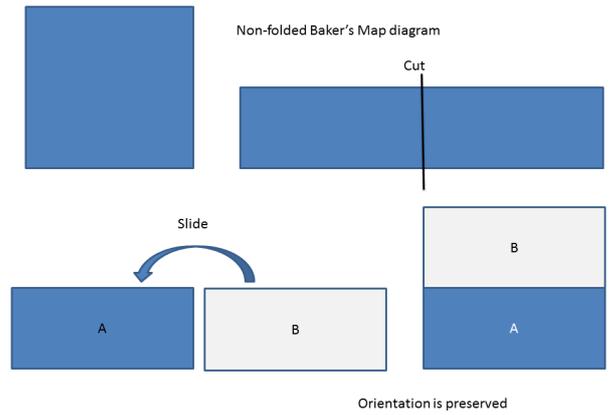
FIG. 8: The "cut and slide" baker's map preserves the orientation of the piece that is moved on top. The transformation involves a stretch and then the right hand piece is moved on top of the other piece.
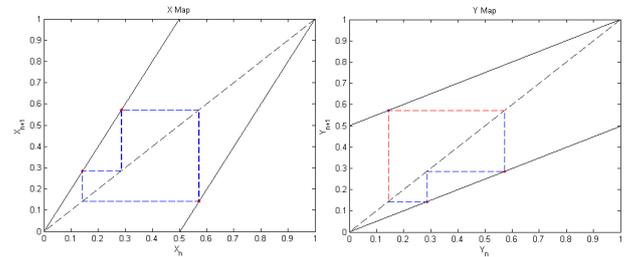

FIG. 9: The periodic orbit 001 for both the X and Y coordinate is displayed here on their respective return maps.

the partitions were colored white and black corresponding with 0 and 1 respectively. In the limit where $n \to \infty$, the evolution of the map will mix the two colors until they are indistinguishably grey.
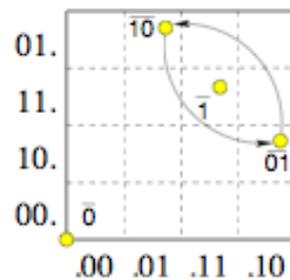

FIG. 10: Partitions of a *knead-and-fold* map. Initial points in periodic orbits *reflect* across y=x

In this way our method of finding periodic orbits of 1-D unimodal maps can be extend to similarly structured maps of the *knead-and-fold* variety. Consider the *knead-*

and-fold quadratic map:

$$x_{n+1} = 1 - 4(x_n - \frac{1}{2})^2$$

$$y_{n+1} = \begin{cases} \frac{1}{2} + \frac{\sqrt{1-y}}{2} & x > \frac{1}{2} \\ \frac{1}{2} - \frac{\sqrt{1-y}}{2} & x < \frac{1}{2} \end{cases} \tag{24}$$

The initial y position of a periodic orbit is equal to the initial x-position of a periodic orbit of the 1-d quadratic map whose label corresponds to the time-order reversed label of our 2-d orbit of interest. For example, the initial position of the 2-D orbit with label 10110.10110 (y.x) is $x_{10110} = 0.8485$, $y_{10110} = x_{01101} = 0.3030$.

With a method in place for finding periodic orbits of 2-D *knead-and-fold* maps, the algorithm for finding the optimal partition of 1-D unimodal maps can be directly adapted to work in 2-D. Pictured below are zeroth-order measures for the periodic orbits of the 2-D quadratic map. The elliptical boundaries indicate the variance of the measure $Q = \begin{pmatrix} \sigma_x^2 & 0 \\ 0 & \sigma_y^2 \end{pmatrix}$. Red ellipses indicate mea-
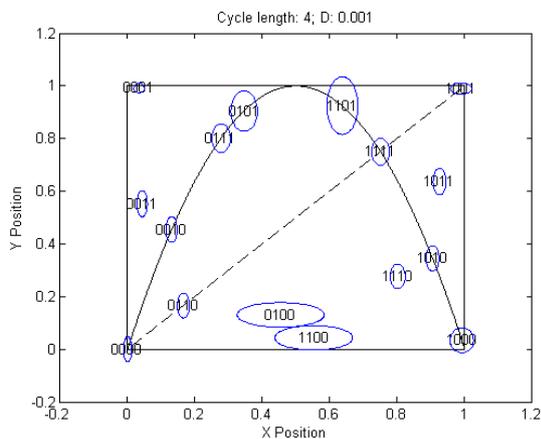

FIG. 11: Zeroth-order measures of the periodic orbits of a quadratic knead-and-fold map. Cycle Length: 4; D=0.001

sures that overlap, meaning they are indistinguishable with the specified noise level.

THE FINAL FRONTIER: HIGHER DIMENSIONS AND WHAT MIGHT BE DONE

The one dimensional case was not horribly difficult to conceptualize. Even the two dimensional case can be rationalized with some effort. Moving beyond these cases becomes difficult. When dealing with a stable system, the covariance matrix is positive and semi-definite. It is not hard to show that the matrix for the forward or adjoint case is invertible. In control theory, the stable and unstable covariance matrices are known as the controllability and observability grammians. Approaching
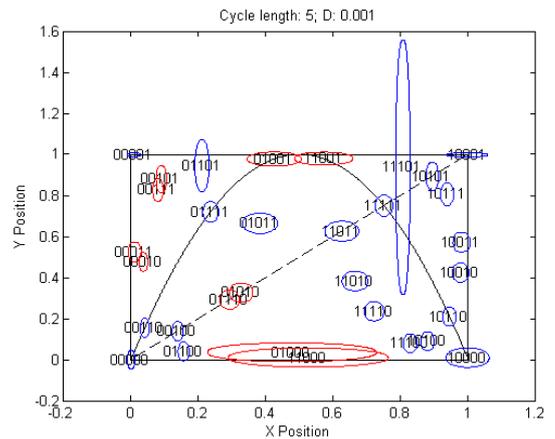

FIG. 12: Zeroth-order measures of the periodic orbits of a quadratic knead-and-fold map. Cycle Length: 5; D=0.001

this we remind ourselves that noise is not isotropic and the resulting covariance matrix is not necessarily a normal matrix. One approach that might be taken is to use singular value decomposition and a similarity transformation.

In order to accomplish this we separate the matrix into it's stable and unstable components. For any system G,

$$G = G_{stable} + G_{unstable} \tag{25}$$

These two components can be independently run through either the forward or adjoint *F-P*.

Following the notes of Cvitanović,

$$Q = MQM^T + \Delta$$

$$Me^{(j)} = \Lambda_j e^{(j)}$$

$$S = \left(e^{(1)}, e^{(2)}, \cdots, e^{(d)} \right) \tag{26}$$

$$S^{-1}MS = \Lambda$$

$$S^T M^T (s^{-1})^T = \Lambda$$

$$\tag{27}$$

$$\hat{Q} \equiv S^{-1}Q(S^{-1})^T$$

$$\hat{\Delta} \equiv S^{-1}\Delta(S^{-1})^T$$

$$\tag{28}$$

The fixed point condition becomes,

$$\hat{Q} - \Lambda Q \Lambda = \hat{\Delta} \tag{29}$$

Each matrix element of Q can be found by calculating,

$$\hat{Q}_{ij} = \frac{\hat{\Delta}}{1 - \Lambda_i \Lambda_j} \tag{30}$$

The equation $Q = S\hat{Q}S^T$ is not a similarity transformation so it remains unclear how the cross terms should be dealt with.

Several papers have explored this question in the field of Controllability. The following is an outline of the methods in these papers for both stable[5] and unstable non-linear systems[6, 7]. In a stable system it can be determined that the Controllability and Observability grammians are

$$W_c = \int_0^\infty e^{At} BB^* e^{A^*t} dt$$

$$W_o = \int_0^\infty e^{At} C^* C e^{At} dt \qquad (31)$$

$$G(s) = C(sI - A)^{-1}B := \begin{bmatrix} A & B \\ C & D \end{bmatrix} \qquad (32)$$

These are solutions of the Lyapunov equations,

$$AW_c + W_c A^* + BB^* = 0$$

$$A^* W_o + W_o A + C^* C = 0$$

$$(33)$$

The Hankel singular values can be defined as,

$$\sigma_i \equiv (\lambda_i(W_c W_o))^{\frac{1}{2}} \qquad (34)$$

A coordinate transform T that sets $\hat{W}_c$ and $\hat{W}_o$ diagonalized and equal is sought.

$$G \sim \begin{bmatrix} T^{-1}AT & T^{-1}B \\ CT & D \end{bmatrix} = \begin{bmatrix} \hat{A} & \hat{B} \\ \hat{C} & D \end{bmatrix} \qquad (35)$$

The grammians in the new coordinates are given by,

$$\hat{W}_c = T^{-1} W_c T^{*-1}$$

$$\hat{W}_o = T^* W_o T$$

$$(36)$$

Now $\hat{W}_c = \hat{W}_o = \Sigma = diag(\sigma_i)$ and we have two relations,

$$(T^{-1}W_c T^{*-1})(T^* W_o T) = \Sigma^2$$

$$T^{-1} W_c W_o T = \Sigma^2$$

$$(37)$$

In this case, it is determined that $W_o = W_o^*$ and is positive definite and can be factored as some $W_o = Y^* Y$ where Y is an invertible matrix. Making substitutions for W_o it is shown that YW_cY^* is similar to Σ^2 and is positive definite. Therefore, a transformation, K, can

be found which preserves the symmetric inner product, $K^* K = \hat{I}$ such that upon substitution,

$$(YT)^{-1} YW_c Y^* (YT) = \Sigma^2. \qquad (38)$$

Simplifying this it can be said that,

$$YW_c Y^* = K\Sigma^2 K^* \qquad (39)$$

with $(YT)^{-1}K\Sigma^{\frac{1}{2}} = \hat{I}$,

$$T = Y^{-1} K\Sigma^{\frac{1}{2}}$$

$$T^{-1} = \Sigma^{-\frac{1}{2}} K^* Y$$

$$. \qquad (40)$$

This transformation sets $\hat{W}_c = \hat{W}_o = \Sigma$.

Approaching this in a nonlinear setting, it cannot necessarily be counted on to have a positive definite matrix. Zhou, et al redefine the observability and controllability grammians as follows.

$$W_c = \frac{1}{2\pi} \int_{-\infty}^{\infty} (j\omega\hat{I} - A)^{-1} BB^* (-j\omega\hat{I} - A^*)^{-1} d\omega$$

$$W_o = \frac{1}{2\pi} \int_{-\infty}^{\infty} (-j\omega\hat{I} - A^*)^{-1} C^* C (j\omega\hat{I} - A)^{-1} d\omega$$

$$(41)$$

In this case the system is restricted to having no poles on the imaginary axis. The system is then,

$$G \sim \begin{bmatrix} T^{-1}AT & TB \\ CT^{-1} & 0 \end{bmatrix} = \begin{bmatrix} A_1 & 0 & B_1 \\ 0 & A_2 & B_2 \\ C_1 & C_2 & 0 \end{bmatrix} \qquad (42)$$

Here A_1 is stable and A_2 is anti-stable. The grammians are composed of W_{o1} and W_{c1}, which correspond to $A_1, B_1,$ and C_1, as well as W_{o2} and W_{c2}, which correspond to $A_2, B_2,$ and C_2. The respective W_o and W_c can be calculated with a transformation,

$$W_c = T^{-1} \begin{bmatrix} W_{c1} & 0 \\ 0 & W_{c2} \end{bmatrix} T^{-1*}$$

$$W_o = T^* \begin{bmatrix} W_{o1} & 0 \\ 0 & W_{o2} \end{bmatrix} T$$

$$(43)$$

By separating the system into its respective stable and unstable grammians and they can be treated with balanced truncation. The Hankel single values remain defined as above. The proof of these relations is done by contour integration. The result is the truncated matrices corresponding to the system,

$$G = G_{stable} + G_{unstable}$$

$$G_{stable} = G_1 = \begin{bmatrix} A_1 & B_1 \\ C_1 & 0 \end{bmatrix}$$

$$G_{unstable} = G_2 = \begin{bmatrix} A_2 & B_2 \\ C_2 & 0 \end{bmatrix}$$

$$(44)$$

In the end, the usefulness of this is determined by how well it can be implemented. For simpler isotropic systems, this may not even be necessary.

[1] D. Lippolis and P. Cvitanovi, Phys. Rev. Lett. **104**, 014101 (2010), URL http://link.aps.org/doi/10.1103/PhysRevLett.104.014101.
[2] D. Lippolis and P. Cvitanovic, *Optimal resolution of the state space of a chaotic flow in presence of noise*.
[3] P. Cvitanović, R. Artuso, R. Mainieri, G. Tanner, and G. Vattay, *http://chaosbook. org* (2008).
[4] H. H. Risken, *The Fokker-Plank equation. Methods of Solution and Applications, SE* (Springer-Verlag, 1989).
[5] *Lectures on dynamic systems and control*, URL http://ocw.mit.edu/courses/electrical-engineering-and-computer-science/6-241j-dynamic-systems-and-control-spring-2011.
[6] K. Fujimoto and S. Ono, in *Decision and Control, 2008. CDC 2008. 47th IEEE Conference on* (IEEE, 2008), pp. 4215–4220.
[7] K. Zhou, G. Salomon, and E. Wu, International Journal of Robust and Nonlinear Control **9**, 183 (1999).

APPENDIX A: ADDITIONAL IMAGES
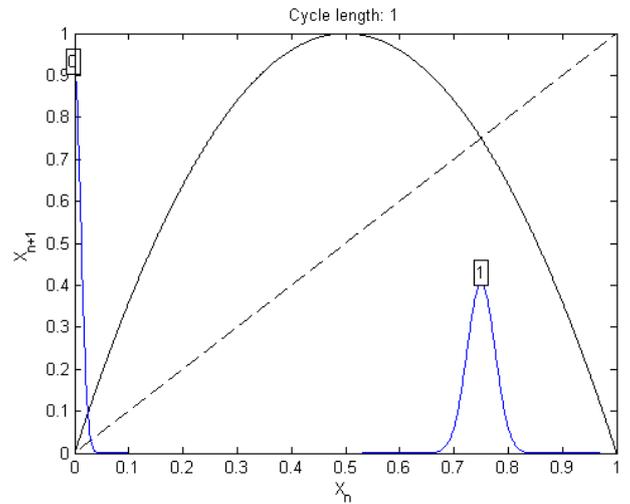
FIG. 13: For the first iteration of the code on the 1-dimensional quadratic map, the separation between cycles of length 1 is well defined.
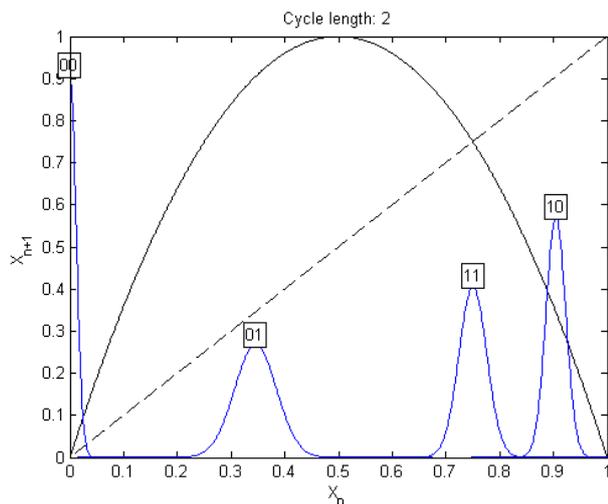
FIG. 14: For the second iteration of the code on the 1-dimensional quadratic map, the separation between cycles of length 2 is still well defined.
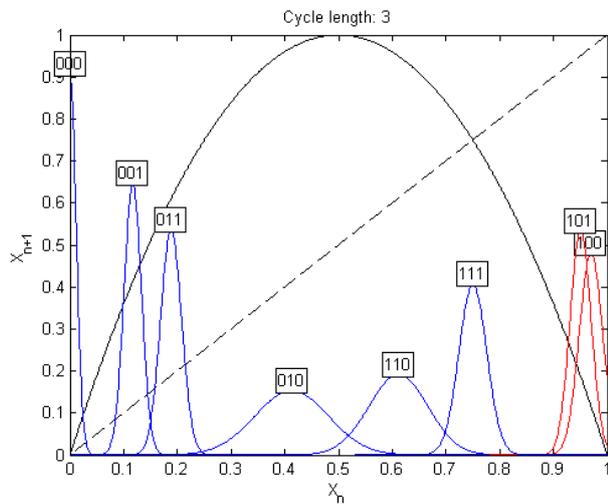

FIG. 15: For the third iteration of the code on the 1-dimensional quadratic map, the separation between cycles of length 3 remains well defined.
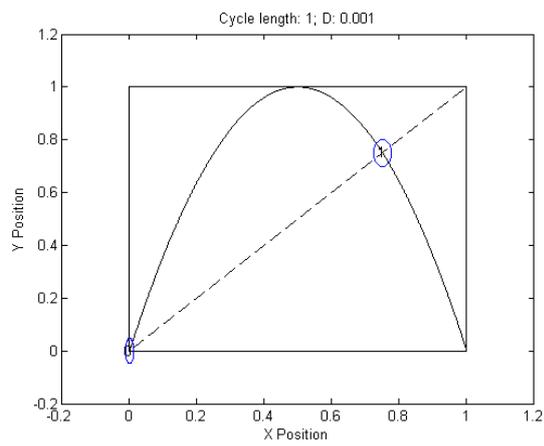
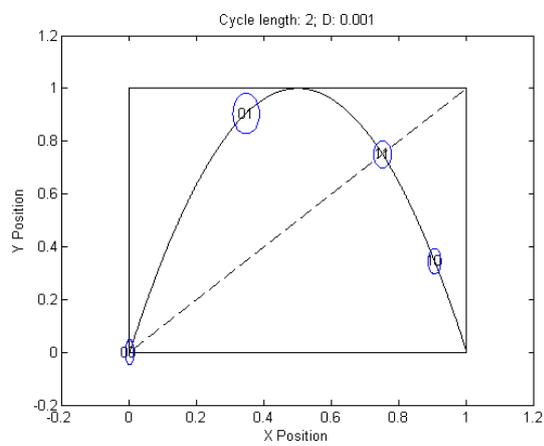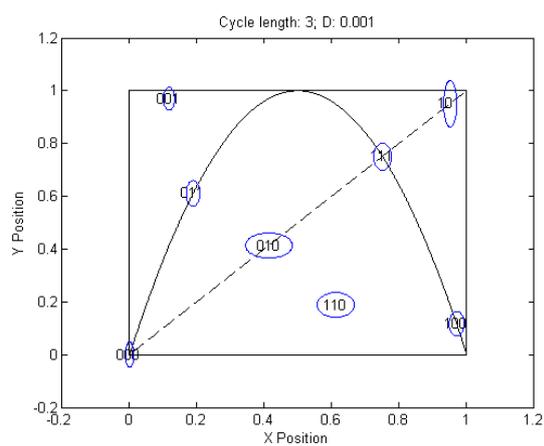FIG. 16: Zeroth-order measures of the periodic orbits of a quadratic knead-and-fold map. Cycle Length: 1; D=0.001

FIG. 17: Zeroth-order measures of the periodic orbits of a quadratic knead-and-fold map. Cycle Length: 2; D=0.001

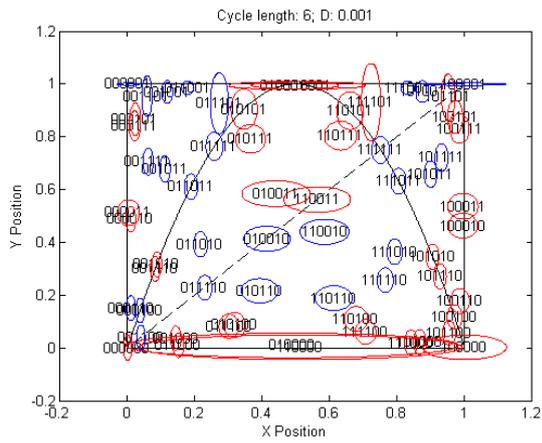FIG. 18: Zeroth-order measures of the periodic orbits of a quadratic knead-and-fold map. Cycle Length: 3; D=0.001

FIG. 19: Zeroth-order measures of the periodic orbits of a quadratic knead-and-fold map. Cycle Length: 6; D=0.001
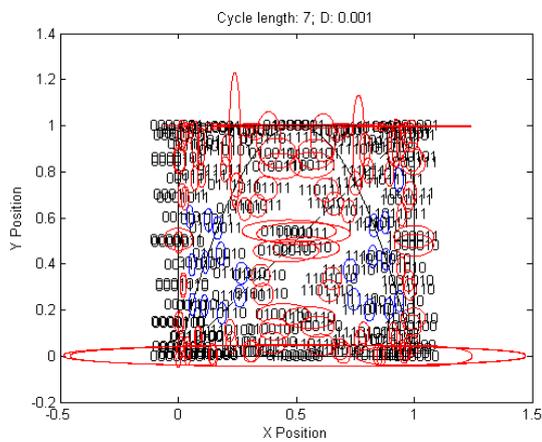

FIG. 20: Zeroth-order measures of the periodic orbits of a quadratic knead-and-fold map. Cycle Length: 7; D=0.001
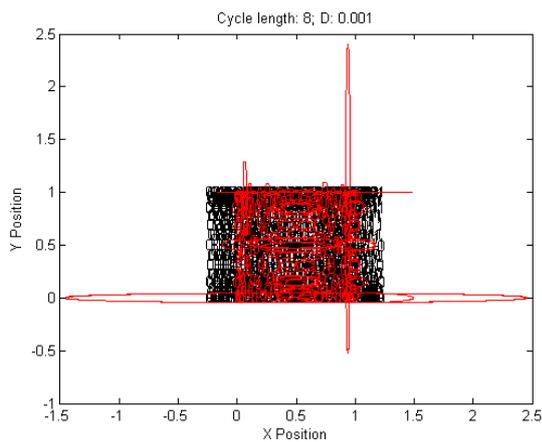

FIG. 21: At this iteration there are no cycles that do not touch. Zeroth-order measures of the periodic orbits of a quadratic knead-and-fold map. Cycle Length: 8; D=0.001